

# DC-Dielectrophoretic separation of biological cells by size

Yuejun Kang · Dongqing Li · Spyros A. Kalams ·  
Josiane E. Eid

Published online: 27 September 2007  
© Springer Science + Business Media, LLC 2007

**Abstract** DC-Dielectrophoresis (DC-DEP), the induced motion of the dielectric particles in a spatially non-uniform DC electric field, is applied to separate biological cells by size. The locally non-uniform electric field is generated by an insulating hurdle fabricated within a PDMS microchannel. The cells experience a negative DEP (accordingly a repulsive) force at the corners of the hurdle where the gradient of local electric-field strength is the strongest. The DC-DEP force acting on the cells is proportional to the cells' size. Thus the moving cells deviate from the streamlines and the degree of deviation is dependent on the cell size. In this paper, we demonstrated by using this method that, combined with the electroosmotic flow, mixed biological cells of a few to tens of micrometers difference in diameter can be continuously separated into different collecting wells. For separating target cells of a specific size, all that is required is to adjust the voltage outputs of the electrodes.

---

Y. Kang · D. Li (✉)  
Department of Mechanical Engineering, Vanderbilt University,  
2301 Vanderbilt Place,  
Nashville, TN 37235, USA  
e-mail: Dongqing.Li@vanderbilt.edu

S. A. Kalams  
Infectious Diseases Unit, Department of Internal Medicine,  
Vanderbilt University Medical Center,  
Nashville, TN 37232, USA

J. E. Eid  
Department of Cancer Biology, Vanderbilt University Medical  
Center,  
Nashville, TN 37232, USA

S. A. Kalams  
Department of Microbiology and Immunology, Vanderbilt  
University Medical Center,  
Nashville, TN 37232, USA

**Keywords** DC-Dielectrophoresis · Cell separation ·  
Microfluidics · Lab-on-a-chip

## 1 Introduction

The cell is the most basic functional element in living organisms. Cells contain important information for genetic development, metabolism, immunological responses, and all other biological processes. Therefore cell separation according to their phenotypes is a fundamental technique in biology and medical biotechnology. Because of their small size ranging from hundreds of nanometers to tens of micrometers, and their dense population, one needs more advanced techniques and subtle devices, instead of traditional tweezers and pipettes, in order to physically access the cells. Thank to the rapid development of lab-on-a-chip technology in the recent decade, researchers can now do cell loading, docking, culturing, sorting, lysis, detection and even single-cell on-chip analysis (Toner and Irimia 2005; Voldman 2006; Dittrich et al. 2006; El-Ali et al. 2006). These cellular lab-on-a-chip devices are not simply scaled-down versions of conventional lab apparatus, they are equipped with various micro- and nanotechnologies. The future of health care may be revolutionized by hand-held analyzers because of their advantages including dramatically reduced consumption of samples and reagents, high speed, integrated functions, automation and portability.

Among the existing techniques for cell manipulations and separation, dielectrophoresis (DEP) may be the most popular method (Gascoyne and Vykoukal 2002; Hughes 2002). DEP arises from the interaction of a dielectric particle, such as a cell, and a spatially non-uniform electric

field. Because electric fields can be scaled down easily at the microscale, a highly non-uniform electric field at a length scale comparable to cell size can be generated at relatively lower voltages. The generated DEP force affects the dynamic behavior of the cells by inducing translational motion or reorientation. Since the relative dielectric polarization (and hence the dielectric response) of the cells depends on the driving frequency of the applied electric field, an alternating (AC) electric-field is usually applied to generate DEP forces of different magnitudes and directions. Therefore DEP devices may be reconfigured for separating other cell phenotypes by modifying field frequency or amplitude. As a common practice in the AC-DEP, an array of metal electrodes is embedded inside a microchannel network to generate a dynamic non-uniform electric field. The micro-electrode structure required for AC-DEP can be fabricated and integrated into the lab-on-a-chip system by conventional photolithographic techniques. Alternatively, static non-uniform electrical fields can be achieved under a DC electric field by specially designed features, such as obstruction or hurdles using electrically insulating materials. Some interesting applications of DC-DEP for particle trapping and concentration in microsystems have been reported recently (Cummings and Singh 2000, 2003; Lapizco-Encinas et al. 2004a, b; Chou et al. 2002; Prinz et al. 2002; Chou and Zenhausern 2003; Ying et al. 2004). The benefits associated with this insulating material based DC-DEP technique are obvious: (1) there is no embedded metal electrode, which greatly reduces the complexity of fabrication by using simple techniques such as soft lithography; (2) the structure is mechanically robust and chemically inert; (3) gas evolution due to electrolysis around the metal electrodes is avoided inside the channel; and (4) DC electric fields can perform both the DEP particle manipulation and the electrokinetic particle transport simultaneously in a microchannel.

It is desirable to explore the practical applications of DC-DEP on particle separation. Recently, the authors proposed a novel method using DC-dielectrophoresis for separation of particles by size (Kang et al. 2006a). In the previous work, we demonstrated that a mixture of polystyrene microparticles of two different sizes can be continuously separated and diverted into two different collecting wells. As a practical application, in this paper, we will show the continuous separation of biological cells by size using the same principle. First we will review the theory of the DC-DEP force affecting the trajectory of cell motion. Then we will describe the experimental design and setup in detail. Finally we will demonstrate the results for separation of human white blood cells and breast cancer cell groups and discuss the limitations associated with the use of electric field in this method.

## 2 Theory

Consider a dielectric particle in an electrically conducting liquid. In the presence of an externally applied electric field, the particles and the surrounding medium are electrically polarized, and the surface charge accumulates at the interfaces due to the difference in electrical permittivity and conductivity of the particle and the liquid. The polarization induces an effective dipole on the particle and the DEP force arises because of the interaction of the particle's dipole and the spatial gradient of the electric field. For an insulating spherical particle of radius  $a$ , in a nonuniform electric field  $E$ , the net DEP force is given by (Pohl 1978; Jones 1995)

$$F_{DEP} = 2\pi\epsilon_f a^3 \tilde{f}_{CM} \nabla |E|^2 \quad (1)$$

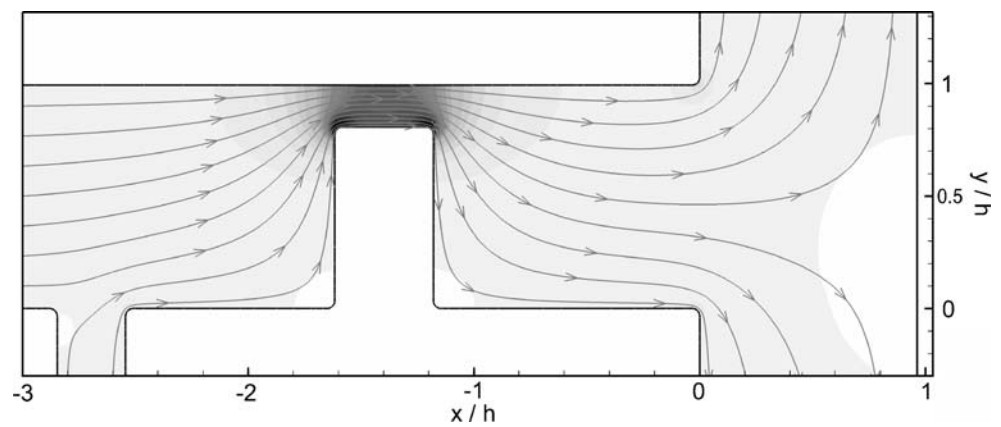
where  $\epsilon_f$  is the electrical permittivity of the suspending medium.  $\tilde{f}_{CM}$  represents the Clausius–Mossotti (CM) factor, which describes the relaxation in the effective polarisability of the particle. The low frequency limiting value of CM factor  $f_{CM} = (\sigma_p - \sigma_f) / (\sigma_p + \sigma_f)$  depends solely on the conductivity of the particle and the suspending medium. Considering the case of insulating particle suspended in a conducting buffer solution,  $\sigma_p = 0$  and  $\sigma_f E \cdot n = 0$ ; the CM factor becomes  $-1/2$ . Accordingly, the net DEP force acting upon a spherical particle reduces to

$$F_{DEP} = -\pi\epsilon_f a^3 \nabla |E|^2 \quad (2)$$

At the low frequency limit, the cell membrane blocks the DC current and causes the cell to behave like an insulating sphere (Jones 1995). Thus expression 2 is also valid for a live cell. It can be inferred from Eq. 2 that the magnitude of the DEP force is proportional to the particle volume ( $4\pi a^3/3$ ) and the gradient of the electric field intensity,  $\nabla |E|^2$ . The negative sign in Eq. 2 implies that the DC-DEP force always directs to the local electric-field minimum. Thus it is also called the negative DEP.

In this work, electroosmotic flow (EOF) of an electrolyte solution is generated inside a microchannel under an applied DC electric field. The liquid properties are assumed to be uniform throughout the channel. Joule heating effects are neglected (Xuan et al. 2004; Erickson et al. 2003). The channel walls are made of electrically insulating materials. A rectangular or triangular hurdle is fabricated in the middle section using the same material. Figure 1 illustrates the electric-field lines and the contours of the electric-field strength  $E$  around the hurdle. Because the total current is conserved in any cross-section of the main channel, the electric field is constricted in the gap region between the hurdle and the channel wall. Thus a stronger and non-uniform local electric field is created near the edges of the hurdle.

**Fig. 1** Distribution of the electric-field lines and contours of the electric-field strength  $E$  around the rectangular hurdle; Darker area has a stronger electric field



By the combined effect of electroosmotic flow (EOF) and the electrophoresis (EP), a suspended particle can move along with the fluid and pass through the gap region. The forces that determine particle trajectories include the dielectrophoretic force, the electrophoretic force, and the Stokes frictional force. In addition there is a dynamic (momentum-associated) component that links the trajectory with particle acceleration, which can be safely neglected because of the particle's micron size. The characteristic time scale for the acceleration phase is about  $10^{-4}$  second, which is of orders of magnitudes smaller than the time scale of the variation of the external forces as well as the time scale of the observation system. Instead of the detailed mathematical formulation, which can be found in the authors' previous publications (Kang et al. 2006a), a brief of the operation principle is outlined here. As shown in Fig. 2, the electric field has a local maximum at the corner of the hurdle. Since the DC-DEP force directs to the local field minimum, the particle experiences a repulsive force when it moves around the corner of the hurdle. The magnitude of the repulsive DEP force is proportional to the particle size. Therefore a larger particle is subjected to a larger DEP force and tends to be deflected to a stream further away from the corner, in comparison with a smaller particle. The similar DEP deflection occurs when the particle passes the corner on the other side of the hurdle. Similarly, particles moving around a triangular shaped

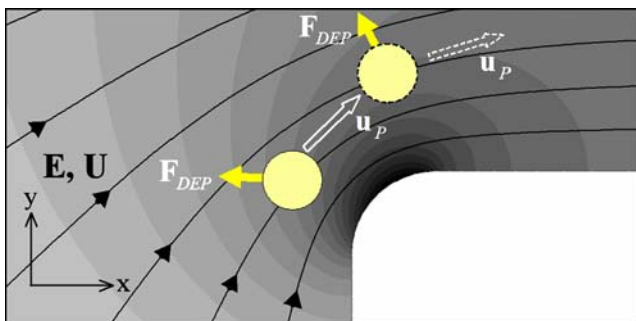


**Fig. 2** DEP force and its effect on a particle near the rectangular hurdle corner. Darker area has a stronger electric field

hurdle also experience the DEP repulsion. As a result, the trajectory deviation because of the DEP deflection will be different for particles of different sizes and hence they can be separated into distinct flow streams. We will show in this investigation that by controlling the electroosmotic flow streams after the hurdle, cells of different sizes can be finally diverted into different collecting wells.

### 3 Experiment

The design of the DC-DEP separation chip and the specific dimension of the microstructure are shown in Fig. 3. There are four branches connected to four different wells. Well B and C are for the cell mixture and the driving buffer solution, respectively. Well A and D are for collecting the separated small and large cells, respectively. Branches A, C, and D are 300  $\mu\text{m}$  in width. Branch B is 90  $\mu\text{m}$  in width. All of the branch channels are 45  $\mu\text{m}$  in depth (in  $z$  direction). The kernel structure is a rectangular hurdle (240  $\times$  130  $\mu\text{m}$ ) or a triangular hurdle (240  $\mu\text{m}$  in base width, 130  $\mu\text{m}$  in height) located between the inputting branches (B and C) and the separation branches (A and D). The PDMS (poly-dimethylsiloxane) microchannel was fabricated following the soft lithography protocol (Duffy et al. 1998). A detailed fabrication procedure can be found in reference (Xuan et al. 2005).

Fixed white blood cells from an HIV-infected subject and the live mammalian breast cancer cells are used individually in the separation experiments. The white blood cells were fixed and supplied in suspension in a lysis buffer (1  $\times$  DMEM, Mediatech, #10-013-CV, Herndon, VA). The solution contains white blood cells (granulocytes, monocytes, and lymphocytes) ranging from 8 to 14  $\mu\text{m}$  and other components (platelets, lysed RBC debris, etc) smaller than 5  $\mu\text{m}$ . The cancer cells (cell line MCF7) range from 20 to 60  $\mu\text{m}$  and were supplied in suspension in nutrition solutions (10 mM Tris, pH 7.5, 50 mM NaCl, 250 mM Trehalose, and 0.02% EDTA). The cell concentration was normally about  $10^6/\text{ml}$ . Since the mass density of the cells are slightly greater than

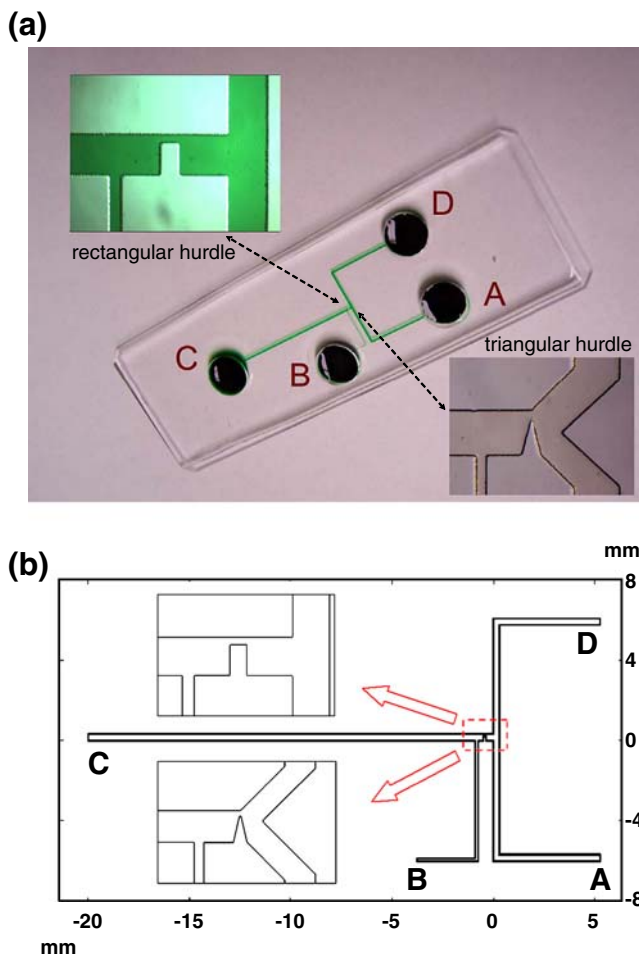


**Fig. 3** Design of the separation chip. (a) Chip design for cell separation; (b) Dimension of the chip and inner structure

that of suspension buffer, the cell solutions were well vortexed prior to use to prevent sedimentation.

In standard protocols for preparation of the nutrition solutions, sucrose instead of trehalose is used. However in this study we have tried both sucrose and trehalose, and found that trehalose gives better protection to the cells under application of the electric field. Under the same situation, the destruction of the cells in trehalose is much lower than in sucrose. This is in accord with the finding by Haritou et al. (2000). They tried eight different sugar media, including sucrose and trehalose, and found that trehalose suppresses the cell destruction (hemolysis) the best, and at the same time it suppresses the cell fusion very well.

Before the experiment, the channel and all the wells were primed with the working buffer (the suspension solutions). Then the cell mixture was introduced into well B with a 1-ml plastic syringe. A high-voltage DC power supply (Glassman High Voltage Inc., High Bridge, NJ) was used to drive the fluid flow through the microchannel network by platinum electrodes submerged in each well. A custom-made voltage controller was used to adjust individ-

ual voltage output of the four electrodes. In the experiments, electrode D was always grounded. The voltage outputs to electrodes A, B, and C were carefully adjusted to ensure that the fluids in the inputting branches B and C always moved towards the hurdle and flowed into the separation branches A and D.

The cell motion was monitored by an inverted optical microscope (Nikon Eclipse TE-2000U) and recorded by a progressive CCD camera (QImaging, Burnaby, British Columbia, Canada). The camera was operated in video mode at a frame rate of 11.4 frames per second. The reading error in determining the particle positions is about  $\pm 2$  pixels which corresponds to actual dimension of  $\pm 5.4 \mu\text{m}$ .

## 4 Results and discussion

### 4.1 Rectangular hurdle for fixed cells

As discussed above, the magnitude of the cell trajectory deviation is proportional to the DEP force acting on the cell, and hence the cell size. Therefore the trajectories of the cells of different sizes can be diverted into different streams after they pass the hurdle. A typical case of separation of fixed white blood cells is shown in Fig. 4, which is obtained by superposing a series of consecutive images of the moving cells. Initially the cell mixture is introduced as a single stream from the inputting branch B. Then the main stream of the buffer solution from branch C pushes the mixture and forces the cells to move closely to the hurdle corner. After the cells pass through the gap between

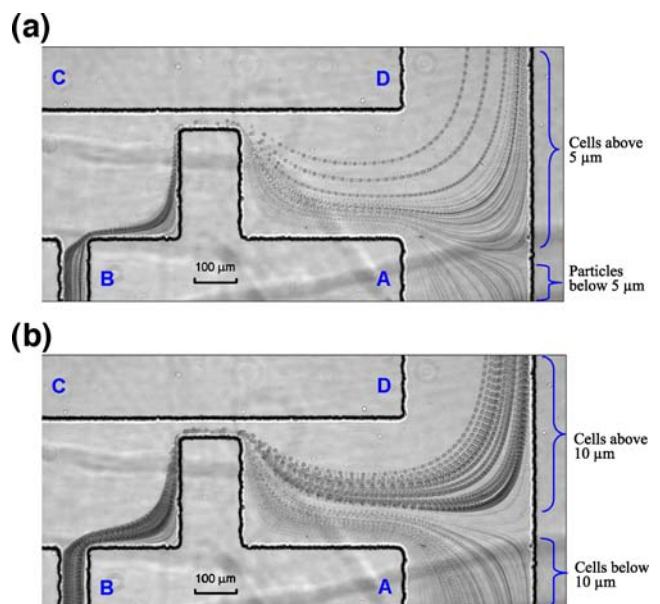


**Fig. 4** Separation of the white blood cells: (a) 5  $\mu\text{m}$  threshold separation,  $V_A=102 \text{ V}$ ,  $V_B=191 \text{ V}$ ,  $V_C=343 \text{ V}$ ,  $V_D=0 \text{ V}$ , and (b) 10  $\mu\text{m}$  threshold separation,  $V_A=62 \text{ V}$ ,  $V_B=191 \text{ V}$ ,  $V_C=343 \text{ V}$ ,  $V_D=0 \text{ V}$



the hurdle and the channel wall, their trajectories changed. The trajectory deviation for a bigger cell is greater than that for a smaller cell or debris because of the different magnitude of the DEP force they experience at the hurdle corners. Thus the single stream of mixed cells is separated into different streams. By adjusting the voltage at electrode A, all of the cells (greater than  $5\ \mu\text{m}$ ) move into branch D, while all the debris of the lysed red blood cells and other small components can be moved into branch A [Fig. 4(a)]. Using a different value of applied voltage at the electrode A, the bigger white blood cells (greater than  $10\ \mu\text{m}$  in diameter) move into the separation branch D, while the smaller cells and debris moves into the other separation branch A [Fig. 4(b)]. In this way, we can purify the cell mixture by removing the lysis debris, or selectively separate the larger cells from the other mixture components. As one of the major advantages, separating target cells of a different size can be realized simply by adjusting the applied voltages. Channel reconfiguration, such as a new design or modified dimensions, is not required.

The highest applied voltage is at electrode C, which determines the overall voltage level of the chip. As pointed out in the previous work (Kang et al. 2006b), maintaining an appropriate voltage level is important to have a high separation speed by enhancing the EOF while avoiding the undesired heating problem. Other than the voltage level  $V_C$ , the voltage output at electrodes A and B are also important to realize the cell separation by size. The applied voltage at electrode A is for controlling the downstream flow streams and hence the cell motion after the hurdle. In this experiment, there exists an effective threshold value of  $V_A$  in order to realize the separation, depending on the specific separation size requirement. For instance, the effective voltage  $V_A$  is about 62 V if one needs to separate cells bigger than  $10\ \mu\text{m}$  [as in Fig. 4(b)]; and  $V_A$  is about 102 V if one needs to remove the debris (particles smaller than  $5\ \mu\text{m}$ ) from the mixture [as in Fig. 4(a)]. The threshold voltages are dependent on the channel configuration and the cell size. They can be easily determined by experimental calibration. The major function of the electrode B in the inputting well is for driving the cell mixture into the hurdle region.

#### 4.2 Improved design: triangular hurdle for live cells

The above design of rectangular hurdle is for separation of the white blood cells, which have been fixed and thus can withstand the strong local electric field for a longer period of time. However, when dealing with the live cells, such as the breast cancer cells used in this study, the narrow constriction gap region between the rectangular hurdle and the channel wall is so long that the live cells passing through it will die. This is because of the extra stress acting on the cell membrane and the induced Joule heating by the

strong local electric field. To minimize the negative effects we modified the design and created a triangular hurdle (as shown in the insets in Fig. 3). In this way, the length of the path where the cells experience the greatest stress is greatly reduced. Meanwhile the required DEP force can still be generated around the tip of the triangular hurdle. To further facilitate diverting the cell streams, we also designed divergent output branches downstream after the hurdle.

Figure 5(a) shows the separation of the white blood cells (greater than  $5\ \mu\text{m}$ ) from the debris. It can be seen that the triangular hurdle works well in terms of separation compared with the rectangular hurdle design (Fig. 4). Furthermore the divergent output branches actually eliminate the stagnant flow area (at the cross of the T-shaped output branches in Fig. 4) created in the previous design, and avoid the problem of slowly moving cells getting stuck in the stagnant region. Figure 5(b) shows the separation of the large breast cancer cells (about  $30\ \mu\text{m}$ ) from smaller

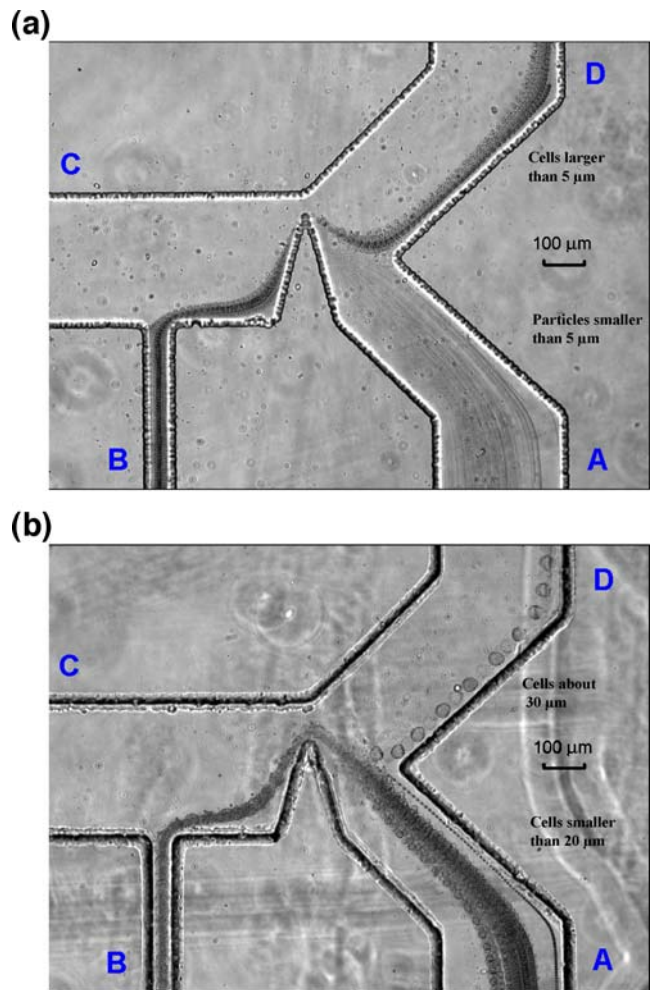


**Fig. 5** Improved design—triangular hurdle with divergent output branches: (a) separation of the white blood cells,  $V_A=31\ \text{V}$ ,  $V_B=136\ \text{V}$ ,  $V_C=345\ \text{V}$ ,  $V_D=0\ \text{V}$ ; (b) separation of the large and small breast cancer cells,  $V_A=56\ \text{V}$ ,  $V_B=154\ \text{V}$ ,  $V_C=180\ \text{V}$ ,  $V_D=0\ \text{V}$

ones (about 20  $\mu\text{m}$ ). Such large cells are thought to represent a subset of mammary stem cells. They constitute a very small portion (less than 1%) of the whole breast cell population. Large breast stem cells are therefore very rare, and this is illustrated in Fig. 5(b) where only one large cell could be detected. The objective of this separation is to isolate stem cells for cell culture and subsequent analyses. To keep them alive after separation, we have to use much lower voltage level [ $V_C=180$  V, Fig. 5(b)] compared with that [ $V_C=345$  V, Fig. 5(a)] for fixed cells.

#### 4.3 Limitations

There are some limitations associated with the DC-DEP separation of the biological cells. Two major problems are the electric field induced membrane stress and the Joule heating. The DEP force is proportional to the gradient of the electric field intensity,  $\nabla|E|^2$ . The electroosmotic flow is proportional to the electric field intensity,  $E$ . Theoretically, application of a higher electric field can generate greater DEP force and stronger electroosmotic flow. However, we observed that live cancer cells die a short time after they are exposed to a very high voltage level, or when they pass through the narrow constriction in the microchannel, i.e., the gap region. This is because the strong DC electric field imposes a great stress on the cell membrane (Voldman 2006). Therefore one cannot significantly increase the voltage to speed up the separation process and to increase the separation efficiency. The other side effect associated with high voltage is Joule heating, which causes significant temperature rise locally and can destroy the channel as well as the biological samples. It is known that a high temperatures (more than 4°C above the cells' physiological temperature) leads to rapid mammalian cell death, and even a less extreme temperature increase may have negative physiological effects (Voldman 2006). In addition, the cell membrane may also be damaged by some free radicals (Feeney and Berman 1976), which can be generated by thermal decomposition and electrolysis at metal electrodes under the application of high voltage. Although some sugars work as free radical scavengers and some enzyme such as catalase and SOD (superoxide dismutase) provide significant protection (Thamilselvan et al. 2000), the temperature elevation because of Joule heating cannot be avoided. Since the viability of the cells after separation is critical for some subsequent analysis, such as the breast cancer cells used in this study, it is highly important to optimize the chip design in order to improve the sample viability. The work presented in this paper is explorative proof of concept. However, much work remains to minimize the negative effects associated with the application of the electric field.

## 5 Summary

DC-Dielectrophoresis is applied to separate white blood cells and breast cancer cells by their sizes. A DC electric field can be used to simultaneously perform both the electrokinetic transport and the DEP separation of cells. The kernel structure is an insulating hurdle between the input and separation microchannel branches, which can generate a local non-uniform electric field. The cell trajectories are deflected by the DEP force around the hurdle, and large and small cells are diverted into different streams. By adjusting the applied voltages at the ends of different branches, a mixture of biological cells of different sizes can be continuously separated into two collecting wells.

This separation method can separate cells with a size difference of a few microns. There exist threshold voltages which are dependent on the desired separation size and channel configuration; they can be easily determined by experimental calibration. The major advantages of this DC-DEP separation are: (1) It can be easily fabricated because the channel geometry is simple. (2) It does not need imbedded microelectrodes inside the channel. (3) The separation is highly efficient and promises high purity of the final samples. (4) Separating target cells of a different size does not require a new channel configuration or modified dimensions. All that is required is a simple adjustment to the applied voltage via the electrodes.

**Acknowledgement** The authors would like to thank the Vanderbilt University for the research grants, and thank Jie Wei and Louise Barnett from Vanderbilt-Meharry Center for AIDS Research for assistance in preparing the fixed white blood cells.

## References

- C.-F. Chou, J.O. Tegenfeldt, O. Bakajin, S.S. Chan, E.C. Cox, N. Darnton, T. Duke, R.H. Austin, *Biophys. J.* **83**, 2170 (2002)
- C.-F. Chou, F. Zenhausern, *IEEE Eng. Med. Biol. Mag.* **22**, 62 (2003)
- E.B. Cummings, A.K. Singh, *Proceedings SPIE*, Santa Clara, CA, 164, (2000)
- E.B. Cummings, A.K. Singh, *Anal. Chem.* **75**, 4724 (2003)
- P.S. Dittrich, K. Tachikawa, A. Manz, *Anal. Chem.* **78**, 3887 (2006)
- D.C. Duffy, J.C. McDonald, O.J.A. Schueller, G.M. Whitesides, *Anal. Chem.* **70**, 4974 (1998)
- J. El-Ali, P.K. Sorger, K.F. Jensen, *Nature.* **442**, 403 (2006)
- D. Erickson, D. Sinton, D. Li, *Lab. Chip.* **3**, 141 (2003)
- L. Feeney, E.R. Berman, *Invest. Ophthalmol.* **15**, 789 (1976)
- P.R.C. Gascoyne, J. Vykoukal, *Electrophoresis.* **23**, 1973 (2002)
- M. Haritou, D. Yova, S. Loukas, *Bioelectrochemistry.* **52**, 229 (2000)
- M.P. Hughes, *Electrophoresis.* **23**, 2569 (2002)
- T.B. Jones, *Electromechanics of Particles* (Cambridge University Press, Cambridge, 1995)
- K.H. Kang, X. Xuan, Y. Kang, D. Li, *J. Appl. Phys.* **99**, 064702 (2006a)
- K. H. Kang, Y. Kang, X. Xuan, D. Li, *Electrophoresis.* **27**, 694 (2006b)

- B.H. Lapizco-Encinas, B.A. Simmons, E.B. Cummings, Y. Fintschenko, *Anal. Chem.* **76**, 1571 (2004a)
- B.H. Lapizco-Encinas, B.A. Simmons, E.B. Cummings, Y. Fintschenko, *Electrophoresis*. **25**, 1695 (2004b)
- H.A. Pohl, *Dielectrophoresis* (Cambridge University Press, London, 1978)
- C. Prinz, J.O. Tegenfeldt, R.H. Austin, E.C. Cox, J.C. Sturm, *Lab. Chip.* **2**, 207 (2002)
- S. Thamilselvan, K.J. Byer, R.L. Hackett, S.R. Khan, *J. Urol.* **164**, 224 (2000)
- M. Toner, D. Irimia, *Annu. Rev. Biomed. Eng.* **7**, 77 (2005)
- J. Voldman, *Annu. Rev. Biomed. Eng.* **8**, 425 (2006)
- X. Xuan, B. Xu, D. Sinton, D. Li, *Lab. Chip.* **4**, 230 (2004)
- X. Xuan, B. Xu, D. Li, *Anal. Chem.* **77**, 4323 (2005)
- L. Ying, S.S. White, A. Bruckbauer, L. Meadows, Y.E. Korchev, D. Klenerman, *Biophys. J.* **86**, 1018 (2004)